


Substituent effects on the Su-Schrieffer-Heeger electron-phonon coupling in conjugated polyenesOliver Stauffert ^{1,2} Michael Walter,^{1,3,4} Mona Berciu,⁵ and Roman V. Krems²¹*Physikalisches Institut, Universität Freiburg, Hermann-Herder-Strasse 3, D-79104 Freiburg, Germany*²*Department of Chemistry, University of British Columbia, Vancouver, British Columbia, Canada V6T 1Z1*³*FIT Freiburg Centre for Interactive Materials and Bioinspired Technologies, University of Freiburg, Georges-Köhler-Allee 105, 79110 Freiburg, Germany*⁴*Fraunhofer IWM, MikroTribologie Centrum μ TC, Wöhlerstrasse 11, D-79108 Freiburg, Germany*⁵*Department of Physics and Astronomy, University of British Columbia, Vancouver, British Columbia, Canada V6T 1Z1*

(Received 13 August 2019; revised manuscript received 17 November 2019; published 19 December 2019)

The Su-Schrieffer-Heeger (SSH) model was introduced to describe the electron-phonon interactions leading to Peierls distortion in polyacetylene (PA). The same model was recently predicted to give rise to unique polaronic effects, including sharp transitions in polaron properties, quasi-self-trapping due to polaron interactions, and the formation of strongly bound yet light bipolarons, at strong electron-phonon coupling in the single and two-polaron limit. This suggests that organic polyenes with strong electron-phonon coupling may exhibit qualitatively different conduction properties from those with weak coupling. In order to observe this, it is necessary to design materials with a range of SSH electron-phonon coupling. Here, we use gradient-corrected density-functional-theory calculations to predict the SSH model parameters for a variety of polyenes, derived from PA by the substitution of the hydrogen atoms with molecular groups. We show that even though the calculations do not accurately reproduce the band gaps, the derivatives of the band structure parameters giving the phonon-induced couplings can be computed with good accuracy. We show that the electron-phonon coupling in such polyenes correlates with the Hammett constant of the substituted molecular group and that some substitutions enhance the coupling strength by as much as a factor of 2. We also find that the electron-phonon coupling in conjugated systems with heavier atoms (such as Si) is much weaker than in PA despite the lower phonon frequencies.

DOI: [10.1103/PhysRevB.100.235129](https://doi.org/10.1103/PhysRevB.100.235129)**I. INTRODUCTION**

Conventional low-temperature superconductivity is known to be mediated by electron-phonon interactions, which induce Cooper pairing [1]. Electron-phonon interactions lead to the formation of polarons (i.e., electrons dressed with phonons). The effective mass of the polarons depends on the type of the electron-phonon coupling. If the coupling modifies the potential energy of the electrons (as described, for example, by the ubiquitous Holstein [2] or Fröhlich [3,4] polaron models), the polaron mass smoothly increases with the coupling strength. The electron pairs dressed by such interactions are also heavy at strong coupling, which has led to the widely accepted conclusion that phonon-mediated interactions cannot be responsible for high- T_c superconductivity [5]. On the other hand, if the electron-phonon coupling modifies the kinetic energy of the electrons (as described, for example, by the Su-Schrieffer-Heeger (SSH) model [6]), the polaron mass undergoes a sharp change and remains low as the coupling strength increases [7]. It was recently shown that the SSH coupling also binds electron pairs into light bipolarons and that the mass of such bipolarons remains low at strong coupling [8,9]. Although the above-mentioned studies were for the limit of single polaron and single bipolaron, they raise the question if bipolaronic high-temperature superconductivity may be possible in materials where the electron-phonon coupling is predominantly of the SSH type.

The SSH model was originally introduced to describe the electron-phonon interactions in the half-filled conduction band of polyacetylene (PA) to explain the structure of PA [6], namely, the bond-length alteration (BLA) and two topologically distinct phases associated with BLA. The SSH model naturally describes the electron-phonon interactions in organic polyenes derived from PA by chemical substitutions of the hydrogen atoms. The prediction of the sharp transition in the properties of the single SSH polaron with increasing electron-phonon coupling suggests that the conduction properties of organic polyenes may be qualitatively different at strong coupling from those at weak coupling. In order to observe this, it is necessary to design materials with a range of the SSH electron-phonon coupling, extending to the strong-coupling regime.

In the present work, we explore the possibility of designing polyenes with a wide range of SSH coupling by modifying PA. We use density-functional-theory (DFT) calculations to analyze the electron-phonon coupling in substituted conjugated polyenes, i.e., polyenes obtained from PA by replacement of the hydrogen atoms with other atoms or molecular groups. The main goal is to determine the effect of the substitutions on the strength of the electron-phonon coupling and the possible range of the coupling strength in polyenes. We predict the electronic properties and the electron-phonon coupling for a range of polyenes and show that the SSH coupling strength is correlated with the Hammett constant of the substituted atomic/molecular group.

II. CALCULATION DETAILS

A. Polaron models

We treat the polyene as a one-dimensional lattice of carbon atoms, each contributing one electron, assume the Born-Oppenheimer (BO) description for the nuclear motion, and describe the nuclear motion with classical displacements $\vec{u}_n = (-1)^n u \vec{e}_x$, where \vec{e}_x is the unit vector along the longitudinal direction and n is the site index of the conjugated chain. The transversal motion of the nuclei is neglected as it affects the electronic degrees of freedom much more weakly. The relevant electronic Hamiltonian including the vibronic couplings can then be written as [6,7]

$$\hat{H} = \sum_n \{ \epsilon c_n^\dagger c_n + [t_0 + 2\alpha(-1)^n u][c_n^\dagger c_{n+1} + c_{n+1}^\dagger c_n] + t'[c_n^\dagger c_{n+2} + c_{n+2}^\dagger c_n] \} + 2KNu^2, \quad (1)$$

where c_n is the operator that removes the electron from site n , ϵ is the on-site energy of the bare electron, t_0 is the nearest-neighbor (NN) hopping amplitude of the bare electron, t' is the next-nearest-neighbor (NNN) hopping amplitude of the bare electron, K is the classical force constant associated with the vibration of the nuclei, α quantifies the electron-phonon coupling strength, and N is the number of lattice sites. For many polyenes, including PA, it is sufficient to consider only the NN hopping and set $t' = 0$. However, as demonstrated below, more complex polyenes require a nonzero t' for an accurate description of the electronic bands.

The parameter α has a simple physical interpretation. In order to describe the electronic Hamiltonian including nuclear displacements, it is not sufficient to use a single constant for the electron hopping parameter. Instead, the hopping t of the electrons from site n to site $(n+1)$ along the vibrating polyene chain must be described as a function of the nuclear coordinates $t = t(\vec{u}_n, \vec{u}_{n+1})$. The electron-phonon coupling α arises from the change of the electronic hopping t due to the displacement. Taylor expanding t and comparing the result with Eq. (1), we can write [6]

$$t(u_n, u_{n+1}) \approx t_0 + \alpha(u_{n+1} - u_n) = t_0 + (-1)^n 2\alpha u, \quad (2)$$

i.e., α determines how the hopping parameter changes with displacement of the carbon atoms in the PA backbone.

To make the notation consistent with the parameters of the model used to compute the properties of polarons and bipolarons in the single polaron/bipolaron limit [7–9], we quantize the phonons and write the phonon part of the Hamiltonian (1) as

$$\hat{H}_{\text{ph}} = \hbar\Omega \sum_n b_n^\dagger b_n, \quad (3)$$

with the vibrational frequency $\Omega = \sqrt{2K/M}$ of the nuclei with mass M , and the electron-phonon interaction as

$$\hat{H}_{\text{el-ph}} = g \sum_n (c_n^\dagger c_{n+1} + c_{n+1}^\dagger c_n)(b_n^\dagger + b_n - b_{n+1}^\dagger - b_{n+1}), \quad (4)$$

where $g = \alpha(2M\Omega)^{-1/2}$. The strength of the electron-phonon coupling can be quantified by the dimensionless parameter

$\lambda = 2g^2/\hbar\Omega|t_{\text{eff}}|$, where $t_{\text{eff}} = t_0 + t'$. This follows the convention to define λ as the ratio of the one-electron ground-state energy with zero hopping to the one-electron ground-state energy with zero electron-phonon coupling. Since the electron-phonon interactions in Eq. (1) are parametrized by α , we express the dimensionless electron-phonon coupling parameter λ in terms of α as follows:

$$\lambda = \frac{2g^2}{\hbar\Omega|t_{\text{eff}}|} = \frac{\alpha^2}{M\hbar\Omega^2|t_{\text{eff}}|} = \frac{\alpha^2}{2K|t_{\text{eff}}|}. \quad (5)$$

The eigenstates $\varepsilon(k)$ of Hamiltonian (1) with $t' = 0$ in the single-particle sector are the energies of the SSH polaron characterized by momentum k . As the electron-phonon coupling λ varies, the SSH polaron dispersion $\varepsilon(k)$ changes as described in Ref. [7]. At some critical value of $\lambda = \lambda_c$, the ground-state properties of the SSH polaron undergo a sharp transition. The critical value λ_c depends on the phonon frequency Ω and approaches 0.5, as $\Omega \rightarrow \infty$. We note that one should not compare the values of λ computed in the presented work directly to the values of λ in Ref. [7] because the results of Ref. [7] are for the single-particle limit and here we consider lattices with half-filled conduction bands. Nevertheless, one can use the value of λ_c from the single-polaron calculations as an approximate indicator of where to expect qualitative changes in the conduction properties of polyenes.

B. DFT calculations

Our goal is to compute the parameters t_0 , t' , Ω , and λ by means of the DFT calculations for a variety of polyenes. The Hamiltonian (1) can be diagonalized to produce the dispersion relation

$$\varepsilon(k) = \epsilon \pm 2\sqrt{[t_0 \cos(ka)]^2 + [2\alpha u \sin(ka)]^2} + 2t' \cos(2ka). \quad (6)$$

The parameters α , $t_{\text{eff}} = t_0 + t'$ (for the lower branch of this band), and K are obtained from the electronic structure calculations, as discussed below. The value of λ is then computed from these parameters using Eq. (5).

The Kohn-Sham eigenvalues in the DFT calculations produce the DFT band structure. In general, this band structure is complex and cannot be described by a model Hamiltonian such as Eq. (1) due to the involvement of many more electrons than assumed in the single state per site tight-binding picture. However, the energies of the highest-occupied (HOMO) and lowest-unoccupied molecular orbitals (LUMO) can be approximated by the eigenvalues of the SSH Hamiltonian. The importance of the SSH description reflects the importance of these orbitals in small perturbations that determine electron transport properties.

When these bands are well described by the eigenvalues of Eq. (1), the values of the polaron model parameters are calculated as follows. As can be seen from Eq. (6), the value of $t_{\text{eff}} = t_0 + t'$ is given directly by the width of the DFT valence band at the center of the Brillouin zone ($k = 0$). To calculate α , we note that

$$\alpha = \frac{\partial t(u)}{2\partial u}. \quad (7)$$

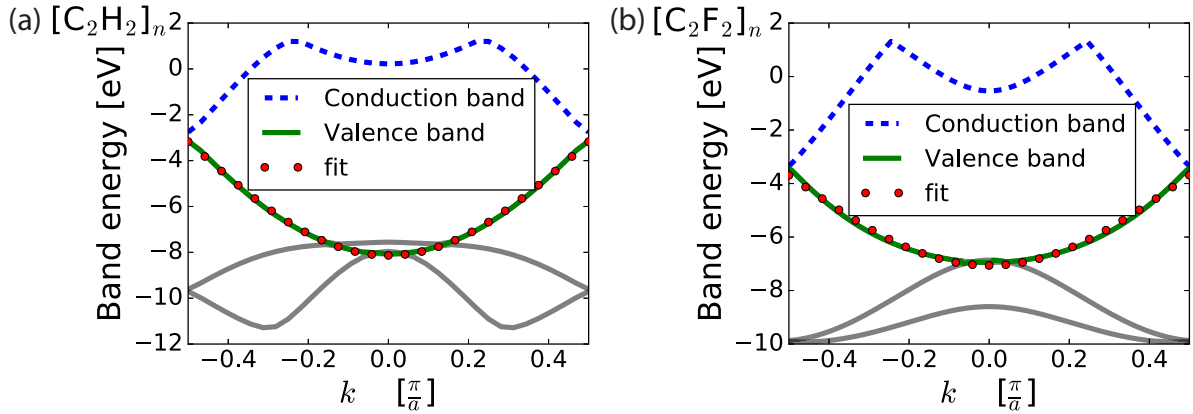


FIG. 1. The band structure of (a) polyacetylene (PA) and (b) H \rightarrow F substituted PA highlighting the bands relevant to the SSH model. The symbols show the values obtained from the fit of the calculated energies for the lower branch of the relevant band (solid green curve) by Eq. (6). Bands of different symmetry intersecting with the valence band are shown in gray.

We calculate the band structure for different displacements $u = 0, \pm 0.001 \text{ \AA}$ and compute the derivative (7) by the finite-difference method. The spring constant $2K$ is obtained by the finite difference of the forces between the backbone atoms of the chain at the equilibrium position. We also note that according to Eq. (6), the band gap δ at the Brillouin zone edge ($ka = \pm\pi/2$) is $\delta = 8\alpha u$ so α can, in principle, be calculated from the band gap. However, as discussed below, the gradient-corrected DFT calculations employed here do not accurately describe the band gap.

The DFT calculations produce a manifold of bands, as illustrated in Fig. 1 for the case of PA and H \rightarrow F substituted PA. We focus on the HOMO and LUMO bands and neglect all bands of different symmetry that cross the bands of interest. In the case of PA, different bands can be clearly assigned to the σ and π orbitals of the carbon chain as there is no coupling between the different symmetries. The valence electrons described by the SSH Hamiltonian are in the π state. The π state is the highest-energy state of the system for most parts of the Brillouin zone, but not at the center. In this case, we use the π state at the center of the Brillouin zone to obtain t_0 . This leads to an accurate description of the valence band with $t' = 0$ both for PA and for its H \rightarrow F substituted variant. If, however, two or more bands exhibit avoided crossings, we use the band of the highest energy throughout the Brillouin zone to describe the valence electrons.

We compute the electronic structure of polyenes by DFT as implemented in the GPAW package [10,11]. The Kohn-Sham orbitals and the electronic density are described within the projector augmented wave (PAW) method [12], where the smooth wave functions are represented by an expansion in plane waves. The plane-wave cutoff for the wave functions was chosen to be 1000 eV. A total of 200 k points are used to sample the Brillouin zone in the periodic direction (x) along the chain with unit-cell length a . Zero boundary conditions are applied in the perpendicular directions and the unit cell is ensured to contain at least 4 \AA of vacuum around each atom in these directions. All structures are allowed to relax without further symmetry restrictions until all forces are found to be below 0.01 eV/ \AA . The optimal unit-cell dimension in x is determined by reducing the strain force to be below 0.005 eV/ \AA .

The exchange-correlation functional is approximated within generalized gradient corrections as devised by Perdew, Burke, and Ernzerhof (PBE) [13].

III. RESULTS

PA has been the subject of many studies and, despite its simple structure, the ground state of PA still challenges theoretical models and experiments [14]. From the molecular structure of PA, one might expect a highly symmetric polymer with fully delocalized π orbital-derived bands resulting in a vanishing band gap. However, this does not agree with the experimental observations, which are more consistent with the presence of bond-length alternation (BLA) due to Peierls distortion [15,16]. The energy gain by BLA was criticized to be below the zero-point level of the corresponding vibration [14,17], further complicating matters. This BLA is well described by the SSH model with parameters given in Table I. The BLA in the SSH model manifests itself in the band gap $\delta = 8\alpha u_0$ between the valence and conduction bands, where u_0 is the displacement in the ground state equal to half the BLA.

A. Phonon dispersions

In the following sections, we consider PA and polyenes derived from PA by the substitution of the hydrogen atoms with other atoms or molecular groups. It is important to consider the effect of this substitution on the phonon energy. We begin by analyzing the phonon dispersions in PA and $[\text{C}_2\text{F}_2]_n$. We calculate the dispersion using a small displacement method

TABLE I. The SSH model parameters for PA and $[\text{Si}_2\text{H}_2]_n$.

Molecule	t_0 (eV)	α (eV/ \AA)	K (eV/ \AA^2)	λ
$(\text{C}_2\text{H}_2)_n$ (present work)	2.56	3.88	16.7	0.17
$(\text{C}_2\text{H}_2)_n$ (SSH model [22])	2.5	4.1	21	0.16
$(\text{C}_2\text{H}_2)_n$ (others) ^a	2.76	4.39	17.8	0.19
$(\text{Si}_2\text{H}_2)_n$	1	0.1	7.39	<0.001

^aDerived from Refs. [16,20,23]; see text.

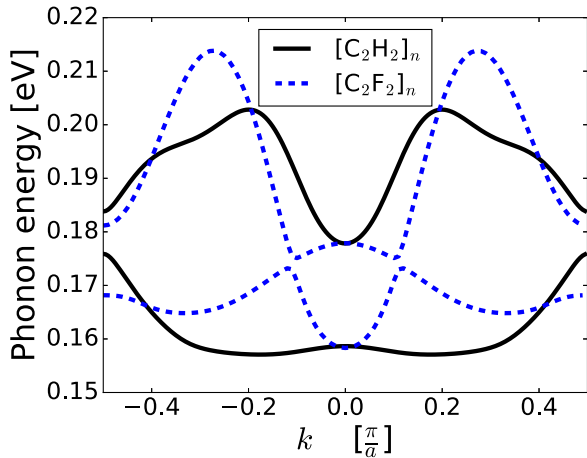


FIG. 2. The dispersion relations for the longitudinal optical phonons in PA $[\text{C}_2\text{H}_2]_n$ (solid curves) and $[\text{C}_2\text{F}_2]_n$ (broken curves).

[18,19]. The results are shown in Fig. 2. Symmetry breaking due to Peierls distortion causes the longitudinal phonons to split into two eigenmodes. The phonon bandwidth of the higher-energy band is 25 meV and the lower-energy band has a bandwidth of 19 meV in our calculations. This is in agreement with the literature results [20,21] showing that the dispersion of the longitudinal phonons in PA relevant for the SSH model is about 20 meV. For the calculation of the parameters of the SSH model in the present work, we use the value of the phonon frequency from the higher-energy band at zero phonon momentum as the value of Ω and neglect the phonon dispersion.

Figure 2 also illustrates the effect of the H \rightarrow F substitution on the phonon bands. The central frequency remains largely unaffected by the substitution, which indicates that the phonon modes arise predominantly from the vibration of the carbon atoms along the conjugated chain. The substitution does affect the vibrational modes corresponding to the transversal motion of the atoms (not shown). They appear as lower-frequency modes for any atom other than hydrogen. However, these modes are coupled to the electronic degrees of freedom much more weakly and are hereafter ignored. This example illustrates our general observation that the phonon frequency Ω relevant for the SSH model (1) is not significantly affected by the substitutions. From this, we assume that the influence of the effective mass of the substituents on Ω is negligible and use the effective mass value from PA for all substituents. We will demonstrate in the subsequent sections that the substitutions affect the value of t_0 and thus alter the electron-phonon coupling significantly.

B. SSH model parameters for $[\text{C}_2\text{H}_2]_n$ and $[\text{Si}_2\text{H}_2]_n$

Table I compares the SSH model parameters for PA derived from our calculations with the available literature data. Calculations of the BLA and the band structure also allow for a reconstruction of t_0 and α . We derived t_0 from half the valence bandwidth calculated via quantum chemistry wave-function methods [23]. Note that the sign of the hopping parameter t_0 if calculated from atomic orbitals is negative [24]. The sign of t_0 , however, does not affect the band structure and is of

no consequence for the present work. Following the original SSH paper [6], we choose t_0 to be positive. The value of α is obtained from the band gap δ and the BLA from PBE0 [16] according to $\alpha = \delta/(4\text{BLA})$. The phonon frequency Ω of Ref. [20] at the Γ point allows for a calculation of $K = \Omega^2 M$, using the effective mass M relevant for the present work.

Gradient-corrected functionals such as PBE used here are known to underestimate the band gap, leading to an underestimate of BLA [16,25,26]. Specifically, the BLA calculated here with the PBE functional is $u_0 = 0.005 \text{ \AA}$ and similarly small values were reported for PBE before [16]. Hybrid functionals were reported to increase this value to an accepted value around $u_0 = 0.08 \text{ \AA}$ [15,16], which roughly agrees with the coupled-cluster results [27], while the BLA calculated from Hartree-Fock methods is known to be overestimated [28].

Despite the underestimation of BLA, the values of t_0 , α , K , and λ , obtained from finite displacements around $u = 0$, are in good agreement with the previous results, as shown in Table I. Correspondingly, our calculations with the same method using the hybrid functional PBE0 [29] lead to $t_{0,\text{PBE0}} = 2.45 \text{ eV}$ and $\alpha_{\text{PBE0}} = 3.75 \text{ eV/\AA}$, i.e., very similar to the PBE results given in Table I. This shows that the derivatives of the energy with respect to the nuclear coordinates, i.e., the forces, are accurately represented by PBE. Exchange and correlation effects not captured by PBE mostly affect electron-electron interactions, which do not strongly depend on the nuclear geometry. All further calculations are therefore performed with the computationally less expensive PBE functional.

The SSH parameters α , K , and t_0 determine the electron-phonon coupling λ . As shown in Table I, for PA, $\lambda = 0.16$. Equation (5) shows that the coupling can be enhanced by increasing the electron-phonon coupling g or, equivalently, α . The value of α can be expected to be larger for electrons that have lower spatial extensions and are closer to the atomic cores as is the case for smaller atoms. This implies that using heavier carbon-isovalent atoms in the conjugated chain, such as Si, should lead to lower α . This conclusion is supported by the results shown in Table I for $[\text{Si}_2\text{H}_2]_n$. Heavier atoms also decrease the phonon frequency as $\Omega \propto M^{-1/2}$. According to Ref. [7], the value of λ_c increases with increasing mass, making it even more difficult to reach the regime of $\lambda > \lambda_c$. Based on this, we exclude polymers with heavy atoms in the conjugated chain from further consideration.

C. Increasing the carbon-carbon bond length

Equation (5) shows that the electron-phonon coupling can be enhanced by reducing the electron hopping energy t_{eff} , provided the other parameters of the SSH model are kept fixed. The magnitude of t_{eff} is determined by the overlap of the electronic orbitals of neighboring carbon atoms so one should expect a decrease of t_{eff} with increasing the C-C bond lengths in the conjugated chain. These bond lengths can be increased by replacing the hydrogen atoms in PA with large molecular groups that introduce steric strain. To obtain insight into the variation of the SSH model parameters with the C-C bond length, we perform model calculations for PA in a stretched unit cell. Figure 3 shows that t_0 is indeed more sensitive to the unit-cell elongation than K or α . Accordingly, λ is generally

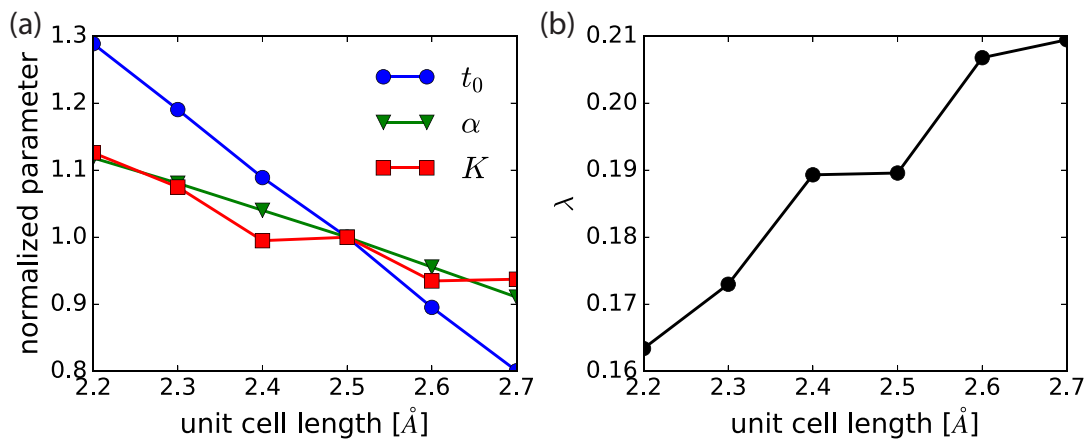


FIG. 3. The changes of the values of the SSH model parameters of PA as functions of the unit-cell length. The parameters in (a) are normalized by the values at equilibrium.

larger for polyenes with longer C-C bonds in the conjugated chain, as illustrated in Fig. 3(b). This is in agreement with the results of Ref. [30] that reported an increased band gap in polymers with applied mechanical strain.

D. Effects of H-atom substitutions

Figures 4 and 5 show the band structures and the SSH model fits by Eq. (6) for several polyenes derived from PA by

the substitution of the hydrogen atoms with different molecular groups similar to these shown in Fig. 1. The model fits accurately describe the HOMO band in all cases. The largest deviations of the numerical results from the model fits occur for NH_2 and NHNO_2 that show a strong maximum at $k = 0$. Table II summarizes the resulting SSH model parameters.

Except for $R = \text{CH}_3$, there is a flattening of the SSH-related band that develops into a maximum at $k = 0$ for some of the substituents. This effect is due to a higher strength

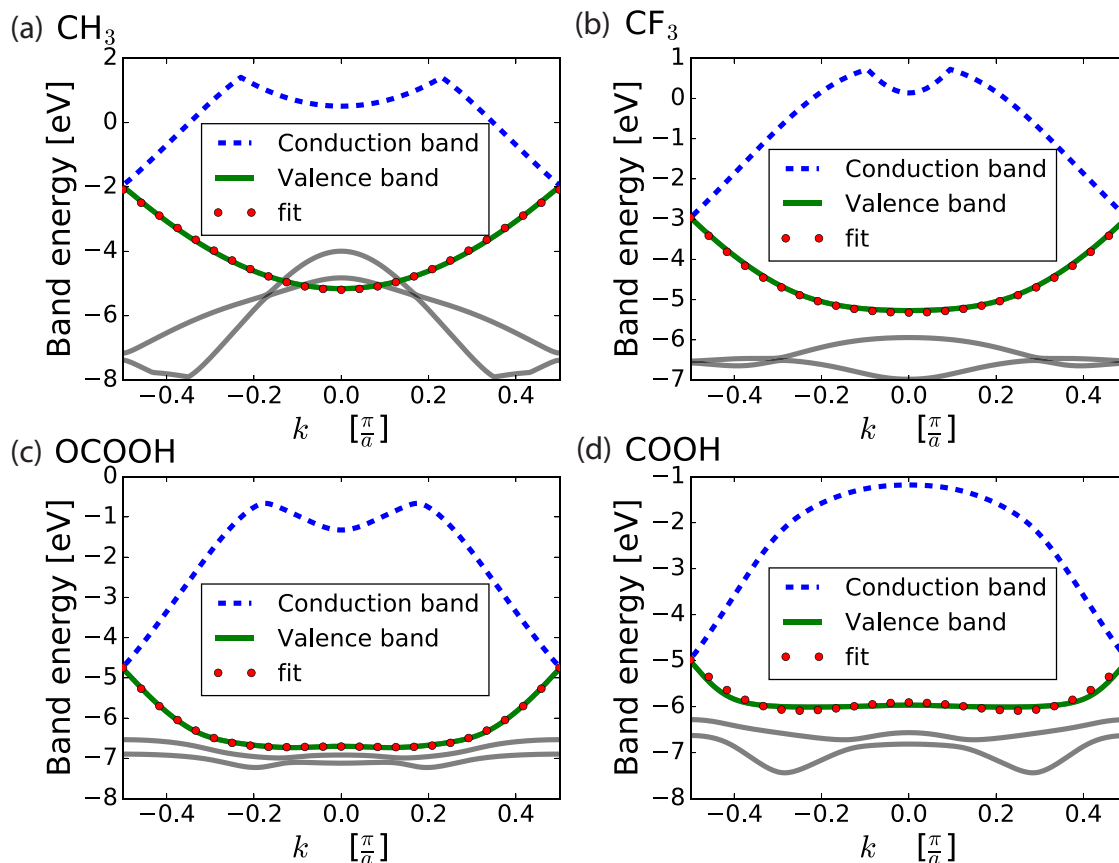
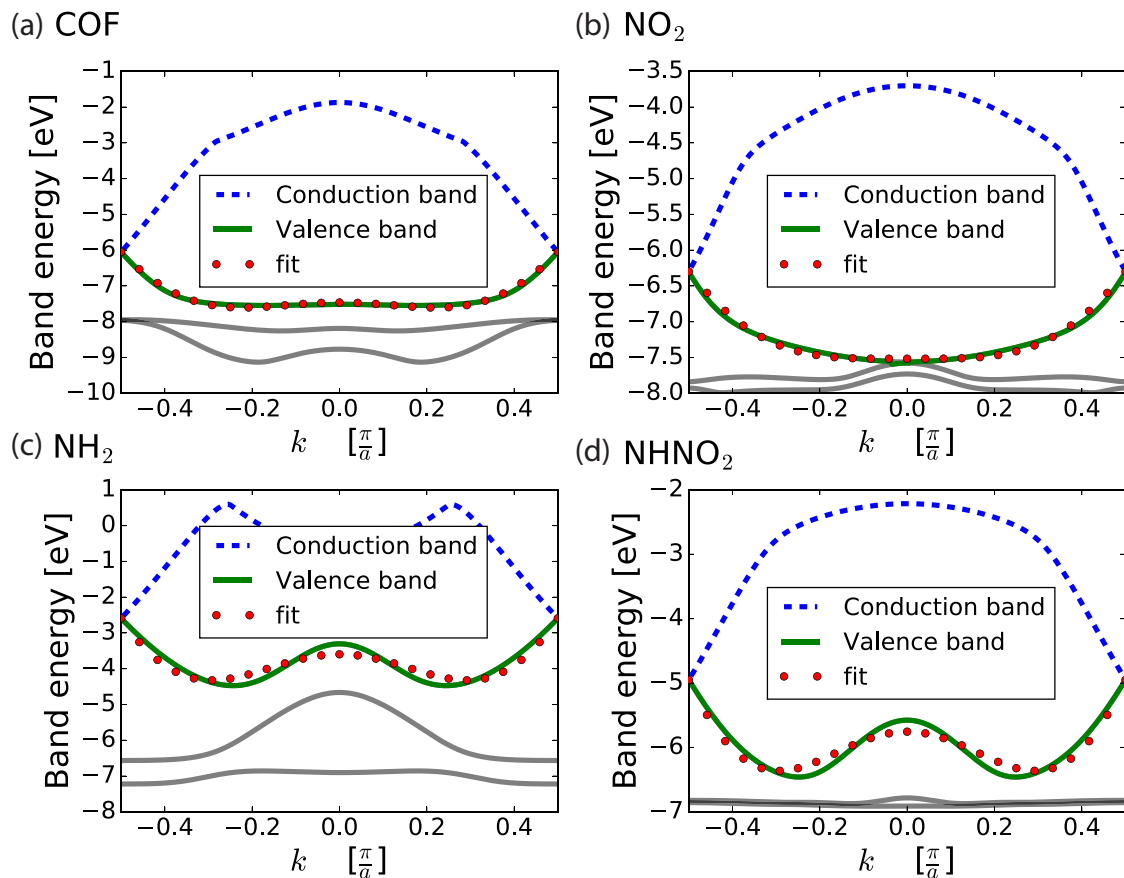


FIG. 4. Electronic band structures in conjugated polyenes $[\text{C}_2\text{R}_2]_n$, with R representing the molecular group indicated on the panels. Solid curves: DFT calculations. Symbols: SSH model fits (6).

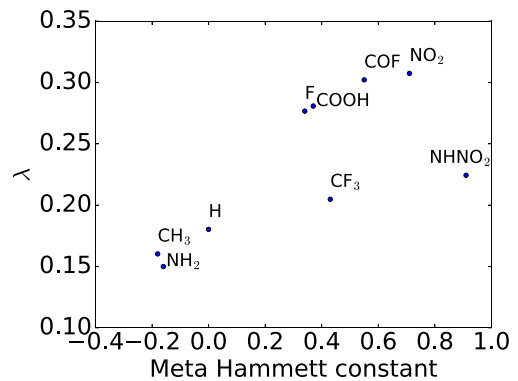

 FIG. 5. Same as in Fig. 4, but for different substituents R .

of NNN hopping, which can be quantified by the ratio t'/t_0 . While t' remains very small under monoatomic substitutions for $R = \text{CH}_3$, some of the substitutions lead to significant values of t' . Increasing the size of the substituents gives rise to stronger NNN hopping, where asymmetric substituents tend to allow stronger NNN hopping. The signs of t' and t_0 appear to be different so the presence of NNN diminishes the effective coupling t_{eff} . No clear correlation can be found between t' and λ . In order to get more insight into the factors that determine the effect of a substitution on the delocalized electrons, we use the Hammett constant [31,32]. This constant characterizes substituents by their effect on aromatic systems [33], which greatly simplifies the choice of substituents for a desired effect

 TABLE II. SSH model parameters for polyenes $[\text{C}_2\text{R}_2]_n$.

$-R$	t_{eff} (eV)	t_0 (eV)	t' (eV)	α ($\frac{\text{eV}}{\text{\AA}}$)	K ($\frac{\text{eV}}{\text{\AA}^2}$)	λ
$-\text{NH}_2$	1.68	2.86	-1.18	2.99	17.7	0.15
$-\text{OCOOH}$	1.76	2.34	-0.58	3.0	17.4	0.15
$-\text{CH}_3$	1.71	1.83	-0.12	3.0	16.4	0.16
$-\text{H}$	2.56	2.56	0.0	3.88	16.7	0.17
$-\text{NHNO}_2$	1.37	2.34	-0.7	2.7	11.5	0.22
$-\text{CF}_3$	1.45	1.74	-0.29	3.21	17.3	0.20
$-\text{F}$	1.79	1.79	0.0	3.87	15.2	0.27
$-\text{COOH}$	1.00	1.53	-0.53	2.9	15.0	0.28
$-\text{COF}$	1.36	2.02	-0.66	3.17	12.2	0.30
$-\text{NO}_2$	0.91	1.21	-0.30	2.72	13.2	0.31

[34]. PA is not aromatic, but it is reasonable to assume a similarity in the delocalized π orbitals to aromatic systems [15]. The Hammett constants for meta and para substitution positions differ and their experimental values are tabulated for a variety of molecular groups [33] or can be obtained from DFT calculations [34]. Figure 6 shows that there is a positive correlation between the meta Hammett constant and the electron-phonon coupling strength λ , with the exception of $R = \text{NHNO}_2$. The para Hammett constant shows similar correlation. Generally, larger values of the Hammett constants lead to higher values of λ . From the list of known Hammett


 FIG. 6. Correlation between the SSH electron-phonon coupling strength λ and the meta Hammett constant for the molecular groups considered in the present work.

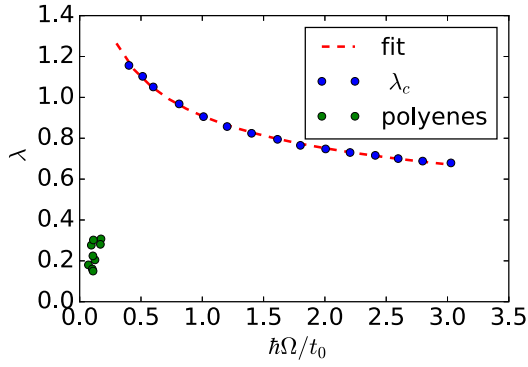


FIG. 7. The values of λ for the polyenes considered in the present work contrasted to the values of λ_c corresponding to the sharp transition in the single-polaron phase diagram (blue circles) from Ref. [7] and a continuous fit following $\lambda_c = A(\hbar\Omega/t_0)^{-\chi}$, with $A = 0.91$ and $\chi = 0.27$.

constants [33], we observe that only bulky or charged substituents have the values exceeding the range considered here. We thus conclude that, in practice, it will be difficult to design a polyene with λ exceeding the range obtained in the present work.

E. Theoretical limit of stretched PA

The values of λ for the polyenes considered here are summarized in Fig. 7. As clearly illustrated, these values are significantly smaller than λ_c for the single-polaron case from Ref. [7] at the corresponding phonon frequency Ω . Stretching the polymer chain may increase λ further, as shown in Fig. 3. However, there is a limit of the stretch imposed by the stability of the carbon-carbon bonds. Here, we attempt to estimate the theoretical limit for the value of λ that can be achieved by stretching PA.

Equation (2) is valid only for small displacements. When the bond is stretched significantly, the expansion must include higher-order terms, which can be generally written as

$$t(u) = \sum_l c_l (-1)^{n-l} u^l, \quad (8)$$

where $c_0 = t_0$ and $c_1 = 2\alpha$. The even terms have a positive sign, while the odd terms have alternating sign. A Fourier transformation into reciprocal space shows that the even terms contribute, to the band structure, a term proportional to $\cos(ka)$, while the odd terms contribute a term proportional to $\sin(ka)$, yielding the dispersion relation for the SSH band,

$$\varepsilon(k) = \epsilon \pm 2\sqrt{[t_0 + c_2u^2 + c_4u^4 + O(u^6)] \cos(ka)]^2 + \{[2\alpha u + c_3u^3 + O(u^5)] \sin(ka)\}^2}. \quad (9)$$

The coefficients in Eq. (8) can be estimated from the dependence of the band energies on u , demonstrated in Fig. 8 for PA. Fitting the SSH band to Eq. (9) leads to $c_2 \approx 6 \text{ eV}/\text{\AA}$.

Figure 8 also depicts the nature of the orbitals corresponding to the bands shown. The two lowest-energy bands are bonding orbitals with symmetry along the carbon chain built from hydrogen and carbon s and $p_{x,y}$ orbitals (assuming the PA chain is in the x, y plane). These bands are only slightly affected by changes in u . The next two bands represent the $p_{x,y}$ bonds with strong bonding character along the direction of the chain x . These bands are strongly affected by changes

in u . While for $|u| < 0.3 \text{ \AA}$ both bonding combinations are occupied, at larger u one of the bonding orbitals becomes energetically higher than the corresponding antibonding orbital. The crossing of the Fermi level by these two bands leads to dissociation of the chain and thus sets the upper limit of attainable displacement to $z = 2\alpha u/t_0 < 0.91$ for PA.

IV. CONCLUSION

The SSH polaron model has recently received much attention due to the predictions of the unique properties of SSH

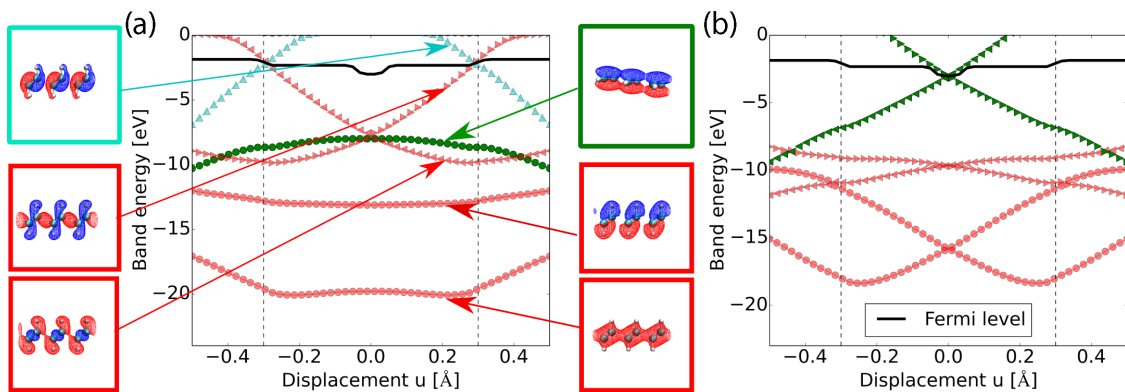


FIG. 8. Single-particle energies at (a) the Brillouin zone center ($k = 0$) and (b) the Brillouin zone edge ($k = \pi/a$) for different displacements u . The band related to the SSH model built from p orbitals perpendicular to the plain is shown in green. Other bands are colored by red and light blue depending on their bonding or antibonding properties, respectively. The orbitals are depicted within three repeated unit cells.

polarons and bipolarons. Of particular interest is the strong electron-phonon coupling regime, where polarons and bipolarons are predicted to exhibit sharp transitions, and where bipolarons are predicted to be strongly bound yet mobile [8,9]. These sharp changes of the polaron and bipolaron properties may manifest themselves in the changes of the conduction properties at finite charge-carrier concentrations and at half filling. Therefore, it is important to design materials with a range of electron-phonon coupling of the SSH type.

The SSH model is known to describe well the delocalized electrons in polyacetylene (PA). However, the SSH coupling in PA is relatively weak. In the present work, we have used gradient-corrected DFT calculations to predict the SSH model parameters for a variety of polyenes, derived from polyacetylene by the substitution of the hydrogen atoms with various molecular groups. We showed that even though the calculations do not accurately reproduce the band gaps, the derivatives of the band structure parameters giving the phonon-induced couplings can be accurately computed. This happens because the electronic energy contributions not captured by the gradient-corrected DFT calculations are only weakly dependent on the translational motion of the carbon nuclei.

We showed that the electron-phonon coupling in conjugated systems with heavier atoms (such as Si) is much weaker than in PA, despite the lower phonon frequencies. This is a

consequence of the fact that the valence electrons are less strongly correlated with the atomic core for atoms with more electronic shells. We also showed that the electron-phonon coupling λ correlates with the Hammett constant of the substituted molecular group and that some substitutions enhance the value of λ by as much as a factor of 2 relative to PA.

We have also estimated the upper limit of λ that can be realized with polyenes with the PA backbone. Unfortunately, the results indicate that this value of λ is far below the value corresponding to the predicted sharp transition in the single-polaron phase diagram. At the same time, many of the λ values obtained in the present work put the polyenes in the range of λ , where interesting bipolaronic physics is expected to occur [8,9]. Our results in Table II are predictions of the SSH model parameters for a wide range of polyenes. These results (and the correlation with the Hammett constant) can be used to inform the experimental design and future theoretical work aiming to understand the role of SSH electron-phonon coupling on the electron conductivity of organic materials.

ACKNOWLEDGMENTS

M.W. thanks Fabian Glatzel for initial studies on polyacetylene. Computational resources of the Freiburg Cluster NEMO are thankfully acknowledged. This work is based on research funded by the DFG through IRTG 2079 CoCo.

-
- [1] L. N. Cooper, *Phys. Rev.* **104**, 1189 (1956).
 [2] T. Holstein, *Ann. Phys.* **8**, 343 (1959).
 [3] H. Fröhlich, H. Pelzer, and S. Zienau, *Lond. Edinb. Dubl. Philos. Mag.* **41**, 221 (1950).
 [4] H. Fröhlich, *Adv. Phys.* **3**, 325 (1954).
 [5] B. K. Chakraverty, J. Ranninger, and D. Feinberg, *Phys. Rev. Lett.* **81**, 433 (1998).
 [6] W. P. Su, J. R. Schrieffer, and A. J. Heeger, *Phys. Rev. B* **22**, 2099 (1980).
 [7] D. J. J. Marchand, G. De Filippis, V. Cataudella, M. Berciu, N. Nagaosa, N. V. Prokof'ev, A. S. Mishchenko, and P. C. E. Stamp, *Phys. Rev. Lett.* **105**, 266605 (2010).
 [8] J. Sous, M. Chakraborty, R. V. Krems, and M. Berciu, *Phys. Rev. Lett.* **121**, 247001 (2018).
 [9] J. Sous, M. Chakraborty, C. Adolphs, R. Krems, and M. Berciu, *Sci. Rep.* **7**, 1169 (2017).
 [10] J. J. Mortensen, L. B. Hansen, and K. W. Jacobsen, *Phys. Rev. B* **71**, 035109 (2005).
 [11] J. Enkovaara, C. Rostgaard, J. J. Mortensen, J. Chen, M. Dułak, L. Ferrighi, J. Gavnholt, C. Glinsvad, V. Haikola, H. A. Hansen, H. H. Kristoffersen, M. Kuisma, A. H. Larsen, L. Lehtovaara, M. Ljungberg, O. Lopez-Acevedo, P. G. Moses, J. Ojanen, T. Olsen, V. Petzold, N. A. Romero, J. Stausholm-Møller, M. Strange, G. A. Tritsarlis, M. Vanin, M. Walter, B. Hammer, H. Häkkinen, G. K. H. Madsen, R. M. Nieminen, J. K. Nørskov, M. Puska, T. T. Rantala, J. Schiøtz, K. S. Thygesen, and K. W. Jacobsen, *J. Phys. Condens. Matter* **22**, 253202 (2010).
 [12] P. E. Blöchl, *Phys. Rev. B* **50**, 17953 (1994).
 [13] J. P. Perdew, K. Burke, and M. Ernzerhof, *Phys. Rev. Lett.* **77**, 3865 (1996).
 [14] B. S. Hudson, *Materials* **11**, 242 (2018).
 [15] M. Kertesz, C. H. Choi, and S. Yang, *Chem. Rev.* **105**, 3448 (2005).
 [16] D.-E. Jiang, X.-Q. Chen, W. Luo, and W. A. Shelton, *Chem. Phys. Lett.* **483**, 120 (2009).
 [17] B. S. Hudson and D. G. Allis, *J. Mol. Struct.* **1032**, 78 (2013).
 [18] Y. Wang, J. J. Wang, W. Y. Wang, Z. G. Mei, S. L. Shang, L. Q. Chen, and Z. K. Liu, *J. Phys. Condens. Matter* **22**, 202201 (2010).
 [19] D. Alfè, *Comput. Phys. Commun.* **180**, 2622 (2009).
 [20] H. Takeuchi, T. Arakawa, Y. Furukawa, I. Harada, and H. Shirakawa, *J. Mol. Struct.* **158**, 179 (1987).
 [21] M. Kofranek, H. Lischka, and A. Karpfen, *J. Chem. Phys.* **96**, 982 (1992).
 [22] W. P. Su, J. R. Schrieffer, and A. J. Heeger, *Phys. Rev. Lett.* **42**, 1698 (1979).
 [23] W. Förner, R. Knab, J. Čížek, and J. Ladik, *J. Chem. Phys.* **106**, 10248 (1997).
 [24] J. C. Slater and G. F. Koster, *Phys. Rev.* **94**, 1498 (1954).
 [25] C. Ho Choi, M. Kertesz, and A. Karpfen, *J. Chem. Phys.* **107**, 6712 (1997).
 [26] J. P. Perdew, *Int. J. Quantum Chem.* **28**, 497 (1985).
 [27] D. Jacquemin and C. Adamo, *J. Chem. Theory Comput.* **7**, 369 (2011).
 [28] V. Bezugly and U. Birkenheuer, *Chem. Phys. Lett.* **399**, 57 (2004).

- [29] J. P. Perdew, M. Ernzerhof, and K. Burke, *J. Chem. Phys.* **105**, 9982 (1996).
- [30] N. A. Lanzillo and C. M. Breneman, *J. Phys. Condens. Matter* **28**, 325502 (2016).
- [31] L. P. Hammett, *Chem. Rev.* **17**, 125 (1935).
- [32] L. P. Hammett, *J. Am. Chem. Soc.* **59**, 96 (1937).
- [33] C. Hansch, A. Leo, and R. W. Taft, *Chem. Rev.* **91**, 165 (1991).
- [34] O. Brügger, T. Reichenbach, M. Sommer, and M. Walter, *J. Phys. Chem. A* **121**, 2683 (2017).